PROCEEDINGS OF SCIENCE

Searches for New Resonances in CMS

Ilias Zisopoulos* **on behalf of the CMS collaboration**

National and Kapodistrian University of Athens,
Zografou Campus 157 72, Athens, Greece

E-mail: ilias.zisopoulos@cern.ch

The quest for new physics is a major aspect of the CMS experimental program. This includes a myriad of theoretical models involving resonances that can decay to massive bosons, photons, leptons, or jets. This talk presents an overview of such analyses with an emphasis on new results and the novel techniques developed by the CMS collaboration to boost the search sensitivity. The searches are carried out using data from Run-II of the LHC in proton-proton collisions with the CMS detector.

The European Physical Society Conference on High Energy Physics (EPS-HEP2025)
7-11 July 2025
Marseille, France

*Speaker

https://pos.sissa.it/

PoS(EPS-HEP2025)424

1. Introduction

The Standard Model (SM) is currently the most successful theory describing the world of subatomic particles, having been confirmed by countless experimental observations. However, it is not yet a complete theory. Many models beyond the SM predict new resonances that decay to massive bosons, photons, leptons, or jets. The analyses presented in this report use proton-proton collision data collected at $\sqrt{s} = 13$ TeV by the CMS experiment [1] at the CERN LHC Run-II period, corresponding to an integrated luminosity of 138 fb^{-1}.

The strategy of these analyses searching for new resonances involves reconstructing the mass of observed final-state particles, modeling the background from SM processes, simulating potential signals, and searching for excesses in the invariant mass spectrum of the beyond-the-SM candidates.

2. Search for heavy scalar resonances decaying to a Higgs and a Higgs-like boson in the Lorentz-boosted $\mathrm{b\bar{b}}$4q final state

Many extensions of the SM predict new heavy resonances X that decay into lighter resonances Y, also beyond the SM, and a SM Higgs boson H. This is the first analysis at the LHC [2] that is searching for X $\rightarrow$ HY processes in final states where H decays into $\mathrm{b\bar{b}}$ and Y into VV $\rightarrow$ 4q, where V denotes a W or Z boson.

The search is conducted in two decay modes: the fully-merged category, where the Y resonance is highly boosted and all four quarks are reconstructed within a single large-radius (AK8) jet; and the semi-merged category, where the two V bosons are resolved individually, each reconstructed as a two-pronged AK8 jet. State-of-the-art jet substructure techniques and taggers are employed to identify such boosted final states. The leading graph-based tagger in CMS, referred to as ParticleNET [3], is used to identify H $\rightarrow$ $\mathrm{b\bar{b}}$ and V $\rightarrow$ qq jets, while the ParT tagger [4], a novel attention-based particle transformer, is used to identify the four-pronged Y $\rightarrow$ VV $\rightarrow$ 4q jet.

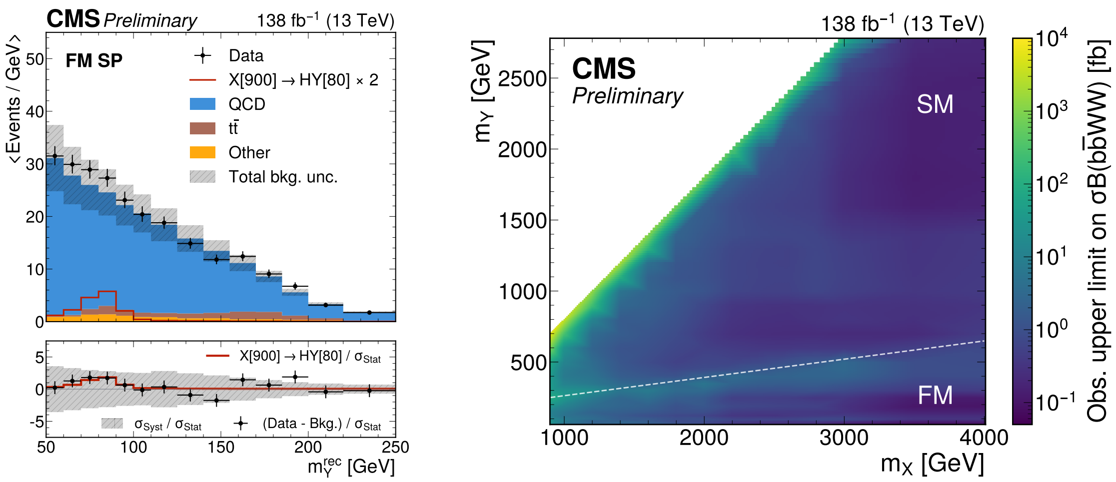

Figure 1: Left: Projected distributions of the $m_{\mathrm{Y}}^{\mathrm{rec}}$ observable in the signal-pass (SP) region of the fully-merged category. Right: Observed upper limits at 95% confidence level on the production cross section times branching fraction for X $\rightarrow$ HY $\rightarrow$ $\mathrm{b\bar{b}}$WW in the 2D m_{X} and m_{Y} plane. Here FM and SM denote the fully-merged and semi-merged categories, respectively. Taken from Ref. [2].

PoS(EPS-HEP2025)424

A 2D maximum-likelihood fit is performed in the reconstructed invariant masses of the X ($m_{\mathrm{X}}^{\mathrm{rec}}$) and Y ($m_{\mathrm{Y}}^{\mathrm{rec}}$) candidates, simultaneously across the signal-pass (SP) and signal-fail (SF) regions, defined by whether the jets satisfy the ParticleNET and ParT discriminants. As shown in Fig. 1 (left), the dominant background in the search is QCD multijet production, which is modeled in a data-driven way using the SF region. Upper limits at 95% confidence level (CL) are set on the $\mathrm{X} \to \mathrm{HY}$ production cross section assuming 100% branching fraction for the $\mathrm{Y} \to \mathrm{WW}$ decays and the SM branching fractions for $\mathrm{VV} \to 4\mathrm{q}$. They are displayed in the 2D m_{X} and m_{Y} plane in Fig. 1 (right).

3. Search for heavy Hγ and Zγ resonances with a b quark pair final state

This analysis [5] targets new heavy resonances, the spin-1 Z′ decaying to Hγ and the spin-0 S decaying to Zγ, with both the Higgs and Z bosons subsequently decaying to a $\mathrm{b\bar{b}}$ pair. Final states with a high-p_{T} isolated photon and a two-pronged AK8 jet are probed, with the AK8 jet identified using the ParT tagger [4]. This novel discriminant outperforms previous taggers used by CMS analyses, achieving the highest signal efficiency for the same background rejection.

Depending on the resonance type, a signal region (SR) is defined by requiring the AK8 jet mass, regressed with ParticleNet [3], to lie within a window around the Z boson mass (SRZ) or the Higgs mass (SRH). Each SR is further divided into a high-efficiency SR (SRZ1, SRH1) and a high-purity SR (SRZ2, SRH2) based on the ParT discriminant score. The invariant mass of the photon and the AK8 jet ($m_{\mathrm{j}\gamma}$) is fit across both SRs for each scenario using six different parametric functions, with the discrete profiling method [6] employed to account for the systematic uncertainty associated with the choice of functional form. Figure 2 shows the data together with the background fits for the SRH1 region. This fitting approach models all SM background processes, with QCD+γ and $\mathrm{Z}+\gamma$ being the dominant contributions.

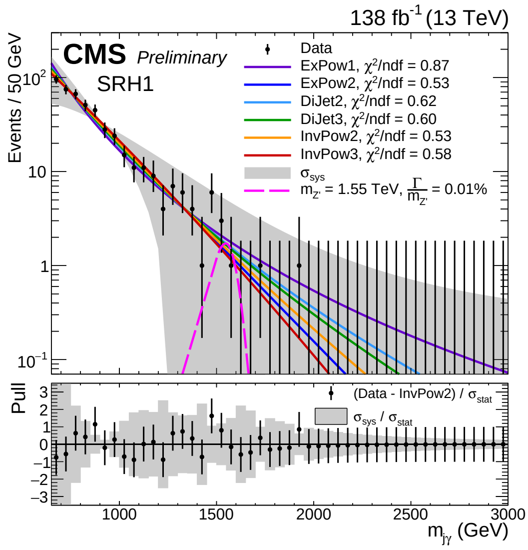

Figure 2: Postfit $m_{\mathrm{j}\gamma}$ spectrum in the SRH1 signal region. The lower panel shows the pull distributions with respect to the best-fit function. A Z′ signal with $m_{\mathrm{Z'}} = 1.55$ TeV, normalized to the observed cross section upper limit, is also shown. Taken from Ref. [5].

Since no significant deviations from the SM are observed, the search sets 95% CL upper limits on the production of narrow Z′ resonances and scalar S resonances with decay widths equal to 0.014, 5.6, and 10% of their mass. The cross section limits on narrow Z′ and S resonances are reported in Fig. 3. As a result of the advanced machine learning techniques employed for jet tagging, these limits are the most stringent to date, representing an improvement by factors of approximately 6–10 compared to previous CMS results [7, 8].

PoS(EPS-HEP2025)424

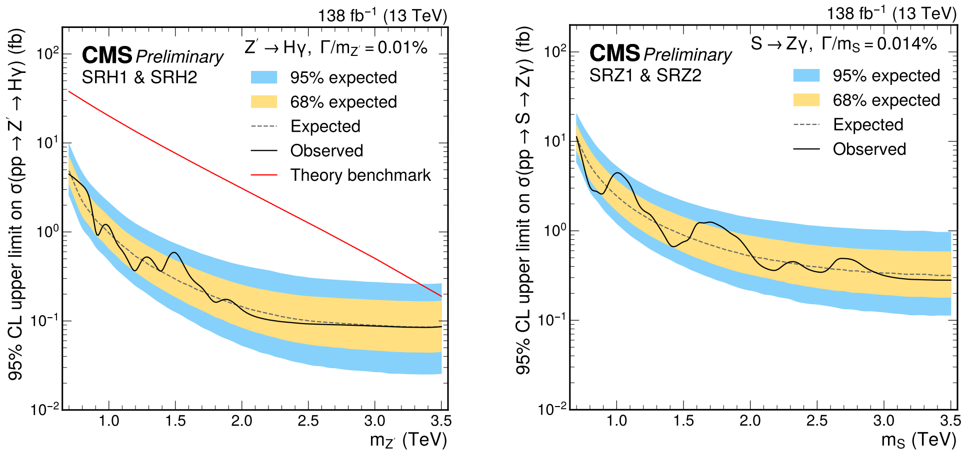

Figure 3: The 95% CL upper limits on the product of cross section and branching fraction for $Z' \to H\gamma$ (left) and $S \to Z\gamma$ (right) with a narrow decay width. Taken from Ref. [5].

4. Search for a heavy resonance produced in association with and decaying to a $t\bar{t}$ pair in the single lepton final state

Motivated by theoretical models predicting Z' resonances that couple exclusively to top quarks [9], this analysis [10] presents the first search of its kind at CMS for a top-philic resonance produced in association with a $t\bar{t}$ pair and decaying to $t\bar{t}$. The search targets the single-lepton channel of the associated $t\bar{t}$ pair, further separated into electron and muon channels. The $Z' \to t\bar{t}$ decay is fully hadronic, producing two AK8 jets that are top-tagged using ParticleNET [3].

The dominant SM backgrounds in this search are top-related and modeled using simulation. A signal-depleted control region (CR) is used to validate the background modeling in the signal region (SR) and to constrain the total background normalization. Figure 4 (left) shows that the background estimation describes the data well.

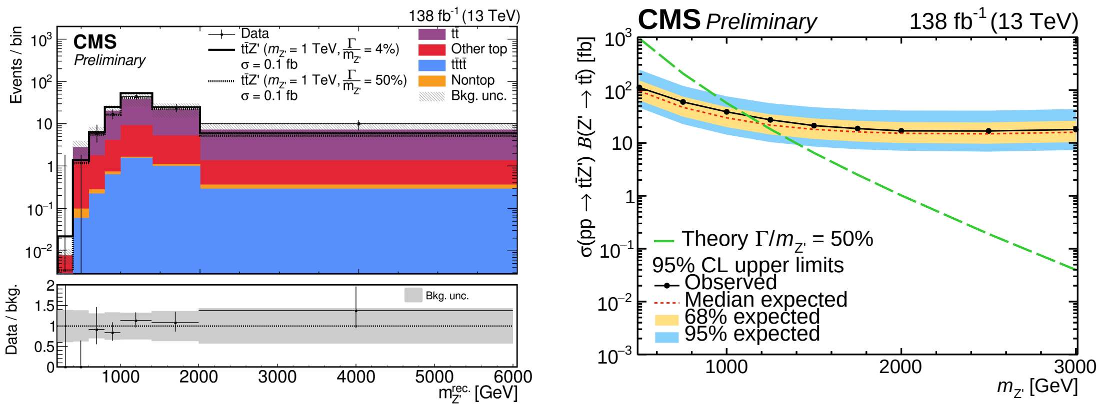

Figure 4: Left: The post-fit distribution of the variable $m_{Z'}^{\mathrm{rec}}$ for the expected background, data, and two Z' signal hypotheses in the signal region for the muon channel. Right: Upper limits on $\sigma(pp \to t\bar{t}Z')\mathcal{B}(Z' \to t\bar{t})$ as a function of $m_{Z'}$ for a Z' resonance with decay width equal to 50% of its mass. Taken from Ref. [10].

A maximum-likelihood fit is performed simultaneously in the electron and muon channels of the

SR and CR, using the reconstructed invariant mass of the Z′ candidate ($m_{Z'}^{\mathrm{rec}}$) as the discriminating variable. Since no excess above the SM prediction is observed, upper limits are set on the production cross section of Z′ resonances with decay widths up to 50%, as shown in Fig. 4 (right). For the model under study, these translate into the most stringent mass limits to date at the LHC.

5. Search for dijet resonances with data scouting

This analysis [11] presents a search for generic narrow dijet resonances in quark-quark ($q\bar{q}$), quark-gluon (qg), and gluon-gluon (gg) final states. The experimental signature is a dijet, composed of two wide jets. Wide jets are formed by taking the two leading AK4 jets in transverse momentum as seeds and combining them with spatially nearby jets satisfying $\Delta R < 1.1$. The jets in this search are reconstructed online at the High-Level Trigger (HLT) from calorimeter information (Calo-jets). A dedicated data stream, referred to as data scouting [12], is used for this purpose, in which only minimal information per event is stored, resulting in smaller event sizes. This enables a higher event rate and substantially lower trigger thresholds. Using data scouting, the dijet resonance mass between 0.6 and 1.8 TeV can be probed, a region previously inaccessible for analyses based on standard data streams [13].

The dominant background arises from QCD multijet production and is modeled by fitting the data directly with a physics-inspired, smoothly falling background function, as illustrated in Fig. 5. The dataset exhibits high statistical precision, making it particularly challenging to fit the full dijet mass spectrum without inducing correlations between the signal strength and the background parameters, which could lead to non-smooth test statistic surfaces. For this reason, the signal is extracted through simultaneous maximum-likelihood fits across subdatasets corresponding to the CMS data-taking periods of each Run-II year.

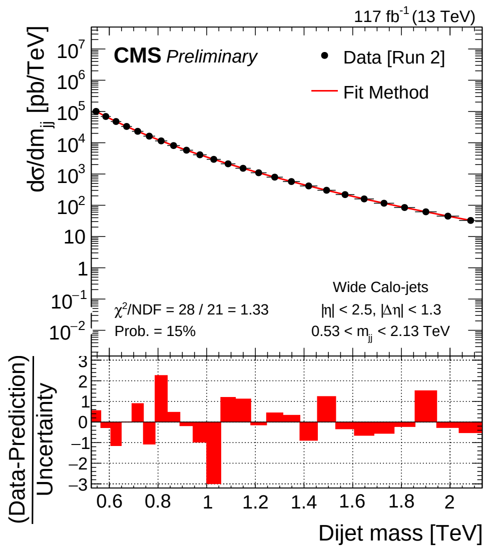

Figure 5: The dijet mass spectrum (points) compared to a fit parameterization of the background (solid curve) for the full Run-II dataset. Taken from Ref. [11].

Model-independent upper limits at 95% CL on the product of cross section, branching fraction, and acceptance are set for the various final states considered, with several benchmark models excluded across the entire mass range. The $q\bar{q}$ final state is shown in Fig. 6 (left).

Limits are also set on the universal quark coupling g'_{q} between a leptophobic Z′ boson and quarks. As shown in Fig. 6 (right), this analysis provides the leading limits in CMS for the mass region probed. The background function in the present analysis has four freely floating parameters, compared to five in the 2016-only CMS result [15], leading to an improvement in sensitivity beyond that expected from luminosity scaling.

PoS(EPS-HEP2025)424

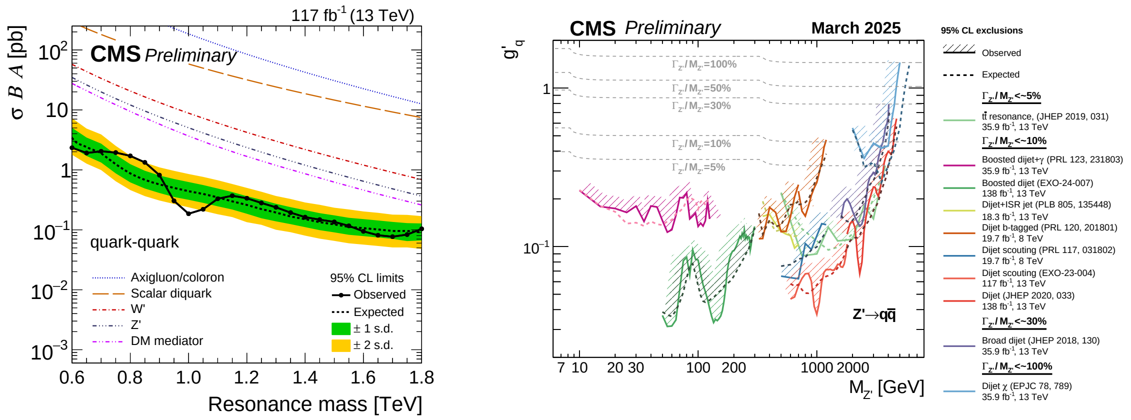

Figure 6: Left: The 95% CL model-independent upper cross section limits for dijet resonances decaying to $q\bar{q}$. Taken from Ref. [11]. Right: Limits on the universal coupling g'_q between a leptophobic Z′ boson and quarks from various CMS dijet analyses. This work is shown with orange lines. Taken from Ref. [14].

6. Search for resonant production of pairs of dijet resonances through broad mediators

This analysis [16] presents a search for resonant production of a pair of identical-mass dijet resonances X, mediated by a particle Y with a broad decay width, ranging from 1.5 to 10% of its mass. It extends a previous CMS search [17], which considered only the case of a narrow mediator with a width less than 0.5% of its mass. The search probes resonant production in both the four-jet and dijet invariant mass spectra, with the 2D distribution of these variables shown in Fig. 7 (left).

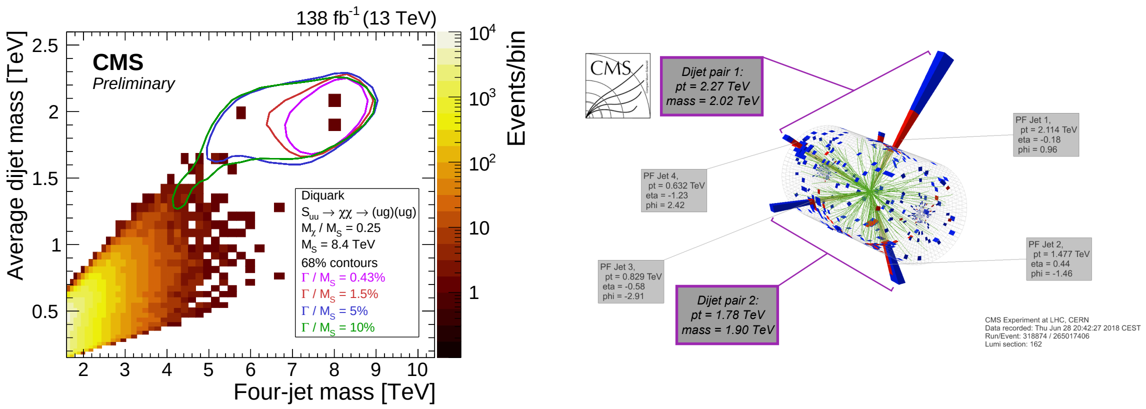

Figure 7: Left: Observed number of events (color scale) within bins of the four-jet mass and the average mass of the two dijets, and the 68% probability contours from a signal simulation of a diquark with a mass of 8.4 TeV, decaying to a pair of vector-like quarks, each with a mass of 2.1 TeV. Right: The 3D display of the event with m_{4j} = 5.8 TeV and $\overline{m}_{2j}$ = 2.0 TeV. Taken from Ref. [16].

There are three events in the tails of the distributions, two with a four-jet mass (m_{4j}) of 8 TeV and one with an m_{4j} of 5.8 TeV, all of which have an average dijet mass ($\overline{m}_{2j}$) of approximately 2 TeV, that result in an excess. Although the event with m_{4j} = 5.8 TeV contributes minimally to a fit with narrow resonances, it is far more compatible with broad resonances of the same mass, as illustrated in Fig. 7 (left). Its 3D event display is shown in Fig. 7 (right). The analysis is further motivated by a similar event with $m_{4\mathrm{j}} = 6.6$ TeV and $\overline{m}_{2\mathrm{j}} = 2.2$ TeV, recorded by the ATLAS Collaboration [18] during the Run-II period.

The signal extraction is carried out through simultaneous signal-plus-background fits to the $m_{4\mathrm{j}}$ distributions, binned in α, where α is defined as the ratio of $\overline{m}_{2\mathrm{j}}$ to $m_{4\mathrm{j}}$. The $m_{4\mathrm{j}}$ spectra are fit with three physics-inspired parametric functions using the discrete profiling method [6].

As shown in Fig. 8 (left), at a four-jet resonance mass of 8.6 TeV and dijet resonance mass of 2.15 TeV, the local (global) significance ranges from 3.9 (1.6) to 3.6 (1.4) standard deviations (s.d.) as the resonance width is increased from 0.43 to 10%. This relative insensitivity to the choice of width indicates that a broad resonance is an equally valid interpretation of this excess. A second excess with a local (global) significance of 3.9 (2.2) s.d. is observed at a four-jet and dijet resonance mass of 3.6 and 1.0 TeV, respectively, for a mediator width of 10%, as shown in Fig. 8 (middle). This excess was previously reported with local (global) significance of 3.6 (2.5) s.d., respectively, in the search for nonresonant production of pairs of dijet resonances [17], and is further discussed in Refs. [19, 20].

Model-independent limits at 95% CL are set on the product of cross section, branching fraction, and acceptance for all mediator widths and a wide range of M_{X} and M_{Y} hypotheses. In addition, mass exclusion limits are derived and presented for $\mathrm{S_{uu}}$ and $\mathrm{S_{dd}}$ scalar diquarks [19, 21–23] decaying to vector-like quarks. The cross section and mass limits for $M_{\mathrm{X}}/M_{\mathrm{Y}} = 0.25$ and a mediator width of 10% are shown in Fig. 8 (right) as a function of the four-jet resonance mass.

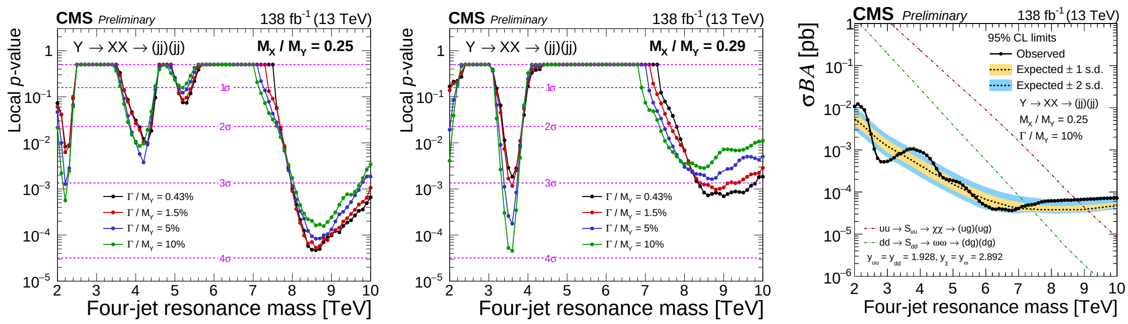

Figure 8: Observed local p-value for a four-jet resonance, Y, decaying to a pair of dijet resonances, X, with $M_{\mathrm{X}}/M_{\mathrm{Y}} = 0.25$ (left) and 0.29 (middle), and various widths of Y superimposed. Right: The 95% CL upper cross section limits for $M_{\mathrm{X}}/M_{\mathrm{Y}} = 0.25$ and width of the resonance Y equal to 10%. Taken from Ref. [16].

7. Summary

A selection of the most recent CMS searches for new resonances has been presented. Several of these analyses employ novel machine learning techniques and advanced taggers to enhance sensitivity and extend the discovery potential beyond previous results, while others probe previously unexplored regions of phase space through dedicated data streams such as data scouting, or push the energy frontier by targeting resonances at the highest accessible masses. Looking ahead, these searches will be further strengthened with larger datasets and higher center-of-mass energy provided by Run-III, for which follow-up analyses are already in progress.

References

[1] CMS collaboration, *The CMS experiment at the CERN LHC*, *JINST* **3** (2008) S08004.

[2] CMS collaboration, *Search for heavy scalar resonances decaying to a Higgs and a Higgs-like boson in the Lorentz-boosted* $\mathrm{b\bar{b}4q}$ *final state*, https://cds.cern.ch/record/2938006.

[3] H. Qu and L. Gouskos, *Jet tagging via particle clouds*, *Phys. Rev. D* **101** (2020) 056019.

[4] H. Qu, C. Li and S. Qian, *Particle transformer for jet tagging*, 2202.03772.

[5] CMS collaboration, *Search for heavy* $H\gamma$ *and* $Z\gamma$ *resonances with a b quark pair final state in proton-proton collisions at* $\sqrt{s} = 13$ *TeV*, https://cds.cern.ch/record/2932616.

[6] P. Dauncey, M. Kenzie, N. Wardle and G. Davies, *Handling uncertainties in background shapes: the discrete profiling method*, *JINST* **10** (2015) P04015.

[7] CMS collaboration, *Search for Narrow* $H\gamma$ *Resonances in Proton-Proton Collisions at* $\sqrt{s}$ = 13 TeV, *Phys. Rev. Lett.* **122** (2019) 081804.

[8] CMS collaboration, *Search for* $Z\gamma$ *resonances using leptonic and hadronic final states in proton-proton collisions at* $\sqrt{s} = 13$ *TeV*, *JHEP* **09** (2018) 148 [1712.03143].

[9] J.H. Kim, K. Kong, S.J. Lee and G. Mohlabeng, *Probing TeV scale top-philic resonances with boosted top-tagging at the high luminosity LHC*, *Phys. Rev. D* **94** (2016) 035023.

[10] CMS collaboration, *Search for a heavy resonance produced in association with and decaying to a tt pair in the single lepton final state in proton-proton collisions at* $\sqrt{s}$= *13 TeV with the CMS detector*, http://cds.cern.ch/record/2929952.

[11] CMS collaboration, *Search for dijet resonances with data scouting in proton-proton collisions at* $\sqrt{s} = 13$ TeV, https://cds.cern.ch/record/2928059.

[12] CMS collaboration, *Enriching the physics program of the CMS experiment via data scouting and data parking*, *Phys. Rep.* **1115** (2025) 678.

[13] CMS collaboration, *Search for high mass dijet resonances with a new background prediction method in proton-proton collisions at* $\sqrt{s} = 13$ *TeV*, *JHEP* **05** (2020) 033 [1911.03947].

[14] CMS collaboration, *CMS Exotica Summary plots for 13 TeV data*, https://twiki.cern.ch/twiki/bin/view/CMSPublic/SummaryPlotsEXO13TeV.

[15] CMS collaboration, *Search for dijet resonances in proton–proton collisions at* $\sqrt{s} = 13$ *TeV and constraints on dark matter and other models*, *Phys. Lett. B* **769** (2017) 520 [1611.03568].

[16] CMS collaboration, *Search for resonant production of pairs of dijet resonances through broad mediators in proton-proton collisions at* $\sqrt{s} = 13$ TeV, https://cds.cern.ch/record/2927625.

[17] CMS collaboration, *Search for resonant and nonresonant production of pairs of dijet resonances in proton-proton collisions at* $\sqrt{s} = 13$ *TeV*, *JHEP* **07** (2023) 161 [2206.09997].

[18] ATLAS collaboration, *Pursuit of paired dijet resonances in the Run 2 dataset with ATLAS*, *Phys. Rev. D* **108** (2023) 112005 [2307.14944].

[19] B.A. Dobrescu, *TeV-scale particles and LHC events with dijet pairs*, *JHEP* **06** (2025) 113 [2411.04121].

[20] A. Crivellin, C.A. Manzari, B. Mellado and S.-E. Dahbi, *Consistency and interpretation of the LHC dijet excesses*, *Phys. Rev. D* **107** (2023) 054045 [2208.12254].

[21] B.A. Dobrescu, R.M. Harris and J. Isaacson, *Ultraheavy resonances at the LHC: beyond the QCD background*, 1810.09429.

[22] B.A. Dobrescu, *LHC probes of the 10 TeV scale*, 1912.13155.

[23] I. Duminica, C. Alexa, I.M. Dinu, B.A. Dobrescu and M.-S. Filip, *Ultraheavy diquark decaying into vectorlike quarks at the LHC*, *Phys. Rev. D* **111** (2025) 115025 [2503.17031].